

Optimizing 3D spectra for rotation control

N.C. Logan¹, S.R. Haskey¹, B.A. Grierson¹, R. Nazikian¹, C. Chrystal², C. Paz-Soldan²

¹ Princeton Plasma Physics Laboratory, Princeton, NJ 08543, USA

² General Atomics, PO Box 85608, San Diego, CA 92186, USA

A new matrix formulation utilizing the multi-modal plasma response to optimize multi-coil spectra for desired neoclassical toroidal viscosity (NTV) torque profiles has been developed in the Generalized Perturbed Equilibrium Code (GPEC) and applied in experimental optimization on the DIII-D tokamak. The new GPEC formulation [1] represents the nonlinear torque as a function of coil array currents, enabling optimization of the coil configurations for maximum, minimum, core localized, and edge localized NTV torque profiles. Experiments have validated this model in non-resonant field space where the braking has little impact on density and energy confinement and is thus ideal for rotation control.

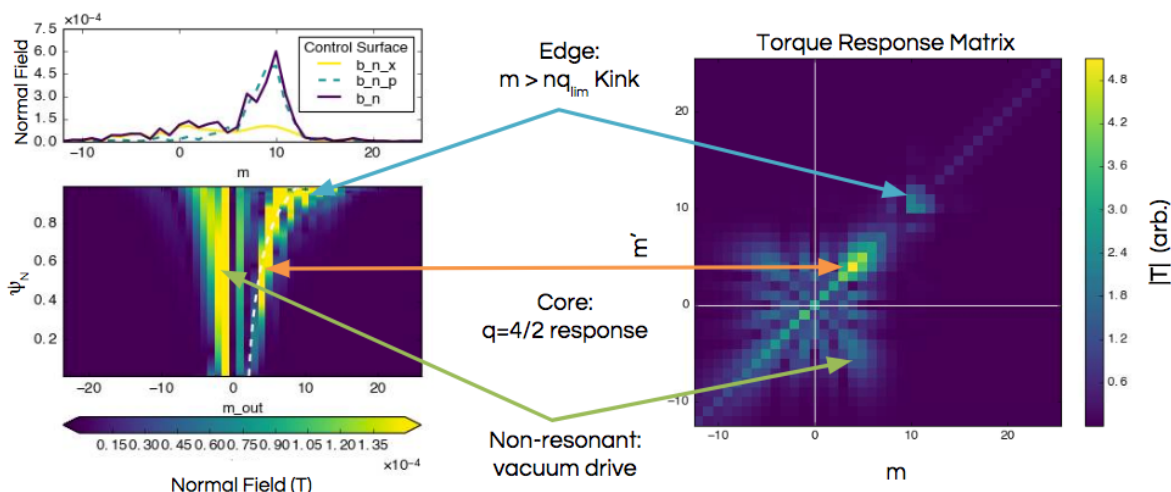


Figure 1: Torque response matrix (right) for DIII-D shot 170433 and normal field of a corresponding perturbed equilibrium driven by 1 kA $n=2$ C-coil currents.

The newly developed GPEC model solves for the perturbed kinetic MHD equilibrium and self consistent NTV torque. The NTV is a second order toroidal torque that comes from the anisotropy of the kinetic pressure tensor. GPEC includes this pressure tensor in the Euler-Lagrange solution when finding the eigenfunctions satisfying force-balance in a numerical method similar to that used in the ideal MHD DCON code [2]. These kinetic MHD eigenfunctions are then used to compile a "torque response matrix" representation of the torque from every coupling between poloidal modes m and m' [1].

This torque response matrix provides insights into the feasibility of NTV profile manipulation. A representative torque response matrix and associated perturbed equilibrium are shown in Fig. 1. In this particular case, there is a large contribution from the core response near the $q = 2$ surface. The torque is also sensitive to the $m \approx q_{95} + 1$ poloidal harmonics, which is correlated with the ideal MHD "dominant mode" [3, 4]. There are also significant contributions from poloidal mode coupling between $m \neq m'$ in the low poloidal mode numbers and significant torque available in the non-pitch-resonant negative m, m' components (this explains the common association between NTV and non-resonant magnetic perturbations).

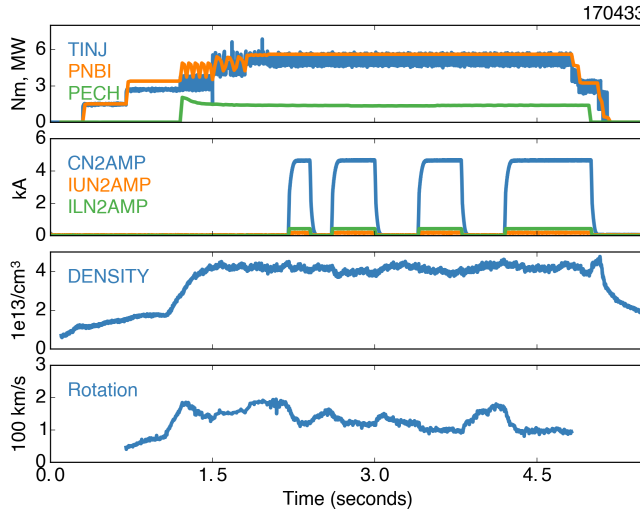


Figure 3: Time series evolution of a representative shot (170433) from this work showing the injected torque and power (top), amplitude of the $n=2$ current each coil array (second), plasma density (third) and edge rotation (bottom).

vides the optimal coil configurations for any desired localized (or total) profiles.

To test the theory, and determine the feasibility of NTV profile control with existing coils, predictions of various NTV profiles were made for the DIII-D ITER Similar Shape (ISS) plasma in which a significant multi-modal plasma response to $n=2$ fields was recently observed [4]. Predictions utilizing the two internal "I" coil and one external "C" coil arrays (each having 6 toroidally distributed coils) were made for the maximum, minimum, edge localized, and core

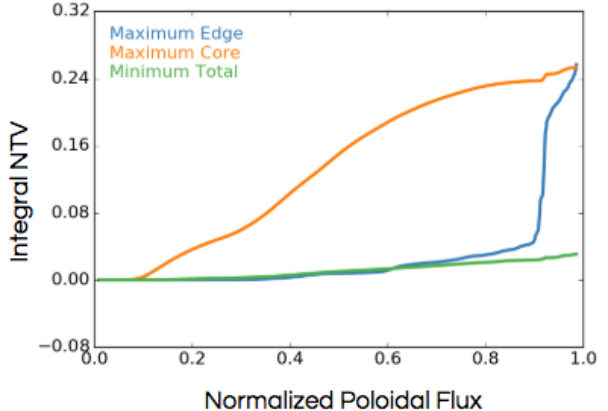


Figure 2: *Localized edge (blue), core (orange), and minimum (green) NTV profiles predicted to be obtainable with the coil arrays on DIII-D.*

Using the plasma response matrix formalization developed for the ideal MHD code IPEC [5, 6], it is possible to form a coil torque response matrix such that the torque T_{NTV} is calculated from the coil currents \mathbf{I}_c by $T_{NTV}(\psi) = \mathbf{I}_c \cdot \mathbf{T}_c(\psi) \cdot \mathbf{I}_c$. With this representation in hand, the optimal coil configuration for localized torque between any two surfaces ψ_1 and ψ_2 is immediately calculable as the first eigenvector and of $\mathbf{T}_{cb}^{-1}[\mathbf{T}_{c1} - \mathbf{T}_{c2}]$, where \mathbf{T}_{cb} is the boundary matrix. A single perturbed equilibrium calculation thus pro-

localized torque as well as for explicitly resonant and non-resonant field configurations. Figure 2 shows that GPEC predicts significant torque profile control within the abilities of the DIII-D coil sets.

The predictions were tested utilizing data from plasma discharges like the example shown in Fig. 3, which had an edge safety factor $q_{95} = 4.2$ and a normalized pressure $\beta_N = 2.5$ with constant beam injection during the flattop. The coils were pulsed on and off with relative $n=2$ coil current amplitudes and phases predicted to induce each of the desired NTV profiles. The dynamic response of the density and rotation were measured and analyzed in OMFIT using 2D fitting and processing methods to ensure smooth spatio-temporal evolution of the transport parameters [7]. An example of the evolution for core (first pulse) and edge (second pulse) NTV coil configurations is shown in Fig. 4.

Experiments validated the core and non-resonant field torque profile predictions, for which the impact of the fields was predominantly on the rotation. Figure 4 shows that the large edge resonant field (which are similar to those used for ELM suppression) cause extensive density pump-out. This significantly distorts the kinetic profiles from the no-field values used in the predictions. The core NTV non-resonant fields cause a much smaller perturbation in the density. Figure 5 compares the experimentally obtained torque profiles to the GPEC predictions for the two pulses shown in Fig. 4 and shows that the experimental NTV torque obtained from the momentum evolution is broad in both cases. The breadth agrees well

with the core NTV prediction but not the sharp edge NTV predicted in the second coil pulse.

In Fig. 5 the experimental NTV profiles are calculated from the angular momentum, neutral beam torque and viscous torque obtained from TRANSP [8]. As TRANSP does not include 3D effects, it adjusts the momentum diffusivity χ_ϕ to increase the viscous torque T_{visc} and maintain torque balance when the coils are turned on and the plasma slows. A simple perturbative model for χ_ϕ is used to reconstruct a corrected viscous torque T_χ [9], and the difference between the

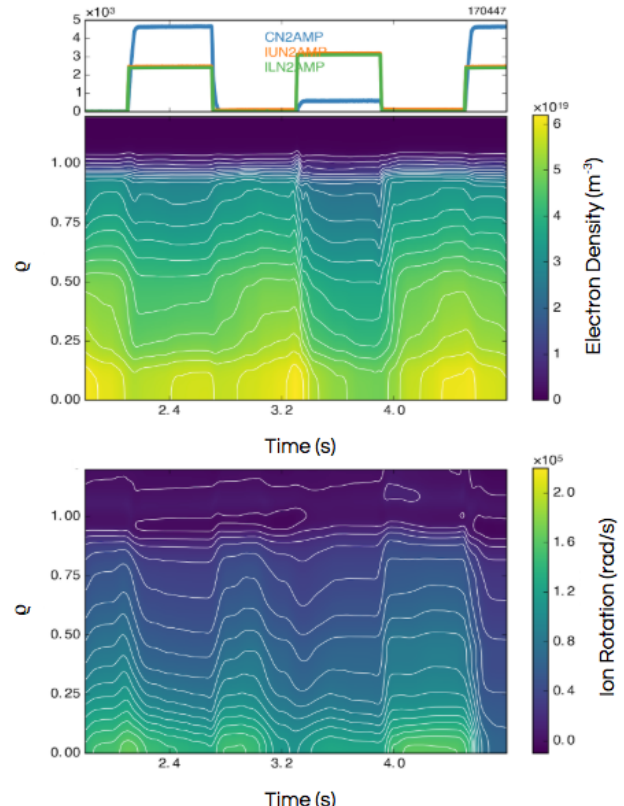


Figure 4: Smooth spatio-temporal evolution of 2D fits for pulsed coil configurations predicted to induce core (first) and edge (second) NTV.

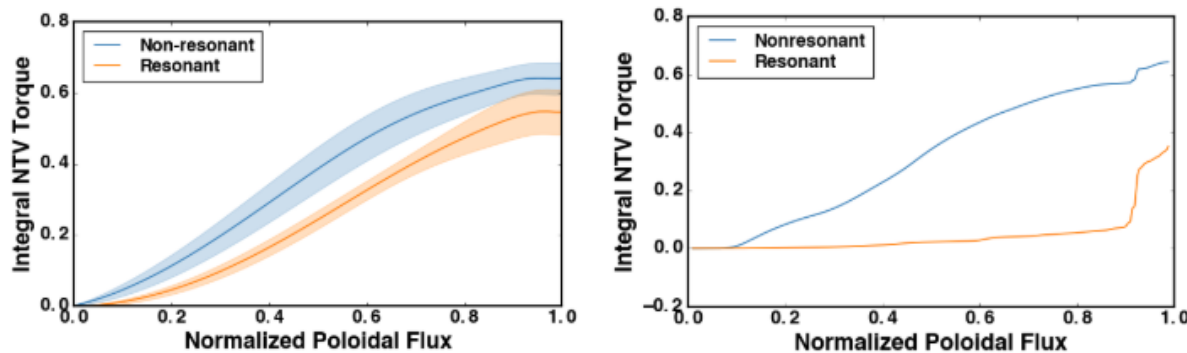


Figure 5: Experimental torque profiles (left) obtained from the momentum evolution during coil pulses shown in Fig. 4 compared to the predicted profiles (left).

TRANSP and reconstructed values is designated the "anomalous" NTV torque, $T_{NTV} = T_{visc} - T_\chi$. In the edge resonant case, broad changes in the density present a dual problem in that they both distort the equilibrium from the modeled state and contribute significantly to the angular momentum evolution being designated as NTV. The result is that the NTV torque calculated in this way is broadly distributed for both the core and edge optimized coil configurations.

Despite the density evolution complications in the edge resonant cases, the experimental application and test of these new GPEC torque matrix predictions represents a significant step towards new practical applications for rotation profile control. The ultimate rotation is clearly impacted differently, and this manipulation using the poloidal 3D field spectrum is a direct application of the multi-mode phenomena [4, 10]. The validated predictions in the non-resonant space provide a path forward for reduced rotation profile control schemes to optimize 3D fields for tokamak stability without sacrificing confinement.

This report was prepared as an account of work sponsored by an agency of the United States Government under awards DE-AC02-09CH11466 and DE-FC02-04ER54698. Neither the United States Government nor any agency thereof, nor any of their employees, makes any warranty, express or implied, or assumes any legal liability or responsibility for the accuracy, completeness, or usefulness of any information, apparatus, product, or process disclosed, or represents that its use would not infringe privately owned rights. Reference herein to any specific commercial product, process, or service by trade name, trademark, manufacturer, or otherwise, does not necessarily constitute or imply its endorsement, recommendation, or favoring by the United States Government or any agency thereof. The views and opinions of authors expressed herein do not necessarily state or reflect those of the United States Government or any agency thereof. DIII-D data shown in this paper can be obtained in digital format by following the links at https://fusion.gat.com/global/D3D_DMP.

References

- [1] J. M. Park et al., Citation: Physics of Plasmas **25** (2018).
- [2] A. H. Glasser, Physics of Plasmas **23**, 072505 (2016).
- [3] J.-K. Park, A. H. Boozer, J. E. Menard, and M. J. Schaffer, Nuclear Fusion **48**, 045006 (2008).
- [4] C. Paz-Soldan et al., Physical Review Letters **114**, 105001 (2015).
- [5] J.-K. Park, A. H. Boozer, and A. H. Glasser, Physics of Plasmas **14**, 052110 (2007).
- [6] J.-K. Park et al., Physics of Plasmas **16**, 056115 (2009).
- [7] N. C. Logan et al., Fusion Science and Technology **0**, 1 (2018).
- [8] R. J. Hawryluk, An Empirical Approach To Tokamak Transport, in *Physics of Plasmas Close to Thermonuclear Conditions*, volume 1, pages 19–46, Brussels: Commission of the European Communities, 1980.
- [9] B. Tobias et al., Physics of Plasmas **23**, 056107 (2016).
- [10] N. C. Logan, C. Paz-Soldan, J.-K. Park, and R. Nazikian, Physics of Plasmas **23**, 056110 (2016).